:≡ **Outline**   📄 **Download**   **Share**   **Export**

Journal of Proteomics
Volume 217, 15 April 2020, 103645

Intermittent fasting from dawn to sunset for 30 consecutive days is associated with anticancer proteomic signature and upregulates key regulatory proteins of glucose and lipid metabolism, circadian clock, DNA repair, cytoskeleton remodeling, immune system and cognitive function in healthy subjects

Ayse L. Mindikoglu [a, b] ⍩ ✉, Mustafa M. Abdulsada [a], Antrix Jain [c], Jong Min Choi [c], Prasun K. Jalal [a, b], Sridevi Devaraj [e], Melissa P. Mezzari [f], Joseph F. Petrosino [f], Antone R. Opekun [a, d], Sung Yun Jung [c, g]

⊞ **Show more**

Get rights and content

open access

Highlights

- First human serum proteomics study of 30-day intermittent fasting from dawn to sunset in healthy subjects

- The 30-day intermittent fasting from dawn to sunset is associated with a serum proteome protective against cancer

- Intermittent fasting from dawn to sunset for 30 days upregulates proteins protective against obesity, diabetes, and metabolic syndrome

☰ Outline   📄 Download   Share   Export

- Intermittent fasting from dawn to sunset for 30 days upregulates proteins protective against Alzheimer's disease and neuropsychiatric disorders

Abstract

Murine studies showed that disruption of circadian clock rhythmicity could lead to cancer and metabolic syndrome. Time-restricted feeding can reset the disrupted clock rhythm, protect against cancer and metabolic syndrome. Based on these observations, we hypothesized that intermittent fasting for several consecutive days without calorie restriction in humans would induce an anticarcinogenic proteome and the key regulatory proteins of glucose and lipid metabolism. Fourteen healthy subjects fasted from dawn to sunset for over 14 h daily. Fasting duration was 30 consecutive days. Serum samples were collected before 30-day intermittent fasting, at the end of 4th week during 30-day intermittent fasting, and one week after 30-day intermittent fasting. An untargeted serum proteomic profiling was performed using ultra high-performance liquid chromatography/tandem mass spectrometry. Our results showed that 30-day intermittent fasting was associated with an anticancer serum proteomic signature, upregulated key regulatory proteins of glucose and lipid metabolism, circadian clock, DNA repair, cytoskeleton remodeling, immune system, and cognitive function, and resulted in a serum proteome protective against cancer, metabolic syndrome, inflammation, Alzheimer's disease, and several neuropsychiatric disorders. These findings suggest that fasting from dawn to sunset for 30 consecutive days can be preventive and adjunct therapy in cancer, metabolic syndrome, and several cognitive and neuropsychiatric diseases.

Significance

Our study has important clinical implications. Our results showed that intermittent fasting from dawn to sunset for over 14 h daily for 30 consecutive days was associated with an anticancer serum proteomic signature and upregulated key regulatory proteins of glucose and lipid metabolism, insulin signaling, circadian clock, DNA repair, cytoskeleton remodeling, immune system, and cognitive function, and resulted in a serum proteome protective against cancer, obesity, diabetes, metabolic syndrome, inflammation, Alzheimer's disease, and several neuropsychiatric disorders. Importantly, these findings occurred in the absence of any calorie restriction and significant weight loss. These findings suggest that intermittent fasting from dawn to sunset can be a preventive and adjunct therapy in cancer, metabolic syndrome and Alzheimer's disease and several neuropsychiatric diseases.

≡ **Outline**   📕 **Download**   **Share**   **Export**
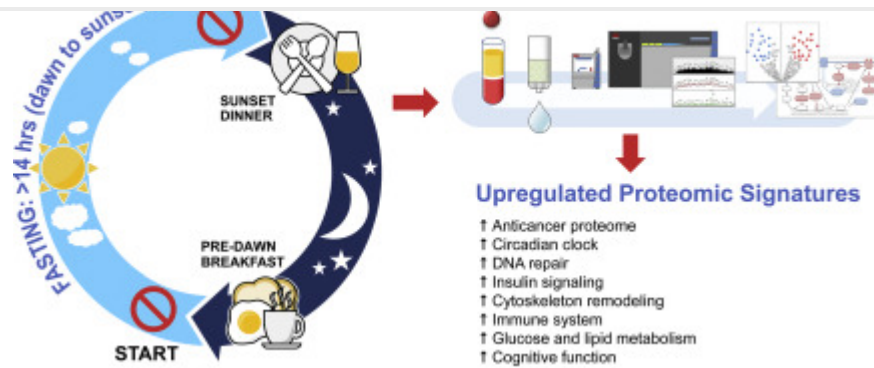
Download : Download high-res image (301KB)   Download : Download full-size image

---

◁ **Previous**   **Next** ▷

1. Introduction

The disruption of circadian rhythm has been associated with alterations in glucose and lipid metabolism and immune system responses, and carcinogenesis [1,2]. Resetting the disrupted rhythm of the circadian clock could be a key strategy in the prevention of metabolic syndrome, immune system dysfunction, and cancer [3,4]. There are two primary mechanisms to reset the circadian clock. The first mechanism functions through the master clock located in the suprachiasmatic nucleus of the anterior hypothalamus that is entrained by dark-light cycles of the day [[5], [6], [7], [8], [9], [10], [11]]. All peripheral clocks are then synchronized by the master clock via neuronal and humoral signals [[5], [6], [7], [8], [9], [10], [11], [12]], and this appears to be the dominant mechanism resetting all peripheral clocks, including hepatic clock during ad libitum food consumption. The second mechanism to reset the circadian clock works in response to mealtime during rhythmic, consecutive, time-restricted feeding-fasting cycles [5,7,10]. Rhythmic consecutive time-restricted feeding-fasting cycles have shown to release peripheral clocks, including the hepatic clock, from the control of the master clock and entrain them independent of the master clock [5,7,10]. Uncoupling of the peripheral clocks from the master clock shifts and resets the phase of the peripheral clocks [5,7,10]. As such, mealtime and duration between meals are critical in resetting and maintaining the circadian rhythmicity of the peripheral clocks [13].

Murine studies showed that time-restricted access or no access to food during night time/dark phase resets the phase of the hepatic clock, optimizes the amplitude of hepatic clock oscillations, and results in the upregulation of mRNA and various protein synthetic pathways, including enzymes that play a crucial role in carbohydrate and lipid metabolism [3,5,7,9,10,14]. Mice are nocturnal feeders; most food consumption and activity occur at night [5,7,9,10,14,15]. In contrast,

☰ Outline   📕 Download   Share   Export

major food consumption at transition zones of the day with a predawn breakfast and dinner at sunset may be as important as caloric content and composition of the food in the prevention of metabolic syndrome and its complications and cancer [13].

Since time-restricted access or no access to food during active phase (night time/dark phase for mice) resets the phase of hepatic circadian rhythm and optimizes the functioning of critical regulatory proteins of metabolism in mice [3,5,7,9,10,14], we formulated and tested the hypothesis that consecutive rhythmic intermittent fasting during active hours (from dawn to sunset for humans) could produce similar optimization in key regulatory proteins protective against cancer, inflammation, metabolic syndrome, and its complications.

2. Methods

2.1. Study subjects

This study was approved by the Institutional Review Board of the Baylor College of Medicine Biomedical Research and Assurance Information Network (BRAIN) under protocol number H-31612 and written informed consent was obtained from all subjects. Inclusion criteria were as follows: 1) Subjects who are 18 years old or older; 2) Subjects who plan to fast during the month of Ramadan [13]; 3) Subjects who are in excellent general health and do not take daily medication for any condition and report no acute illnesses or symptoms at the time of enrollment. Subjects were excluded if they had any of the following: 1) Body mass index equal to or >30 kg/m^2; 2) History of acute, sub-acute, or chronic disease; 3) Use of any daily medications (occasional use of over-the-counter medications to relieve pain, such as acetaminophen or ibuprofen, in minimal to moderate amounts, was permitted); 4) Use of alcohol or recreational substances.

2.2. Study procedures

A 1-hour screening visit was scheduled within 12 weeks of initiation of 30-day intermittent fasting at Baylor College of Medicine in the Texas Medical Center Digestive Diseases Center Clinical Research Core E Laboratory. During this visit, the subjects' eligibility was assessed based on inclusion and exclusion criteria, and written informed consent was taken. Medical history and physical examination were performed. Urine pregnancy for the female subject at childbearing age was performed.

Daily fasting began at dawn after a predawn breakfast and ended at sunset with a dinner for 30 consecutive days. Fasting occurred without eating or drinking between predawn breakfast and dinner at sunset (lunch, liquids, water, snacks were skipped). There was no calorie restriction,

Outline   Download   Share   Export

Blood specimens for biomarkers and proteomic analysis were collected within four weeks before the initiation of 30-day intermittent fasting after an overnight fast, at the end of 4th week during 30-day intermittent fasting after at least 8 h of fast, and one week after completion of 30-day intermittent fasting after an overnight fast.

To confirm future compliance during the study (a daytime rise in enrichment indicates non-compliance to fasting), a baseline ^{13}C-isotopic breath enrichment test as described by Opekun et al. [16] was performed within four weeks before 30-day intermittent fasting (baseline). Thereafter, ^{13}C-isotopic breath enrichment samples were collected throughout the study until the end of 30-day intermittent fasting to assure protocol compliance during the study.

2.3. Serum proteomics

Several methods of serum sample preparation were tested, as shown in Fig. 1 to establish a workflow to get the best peptide and proteome coverage. Each of these methods utilized 10 μl volume of serum. For the non-depleted serum samples, 10 μl serum was subjected directly for S-Trap aided digestion method. The peptides were resuspended in ultra high-performance liquid chromatography (HPLC) loading buffer (5% MeOH, 0.1% FA) and subjected to nLC1000 coupled Orbitrap Elite. For the top 12 abundant protein depletion, 10 μl of serum was incubated with the resin slurry of the depletion kit (Thermo Scientific Pierce, Cat# 85164) for an hour at room temperature followed by digestion on S-Trap column (ProtiFi, NY). The S-trap column aid digestion was carried out using the trypsin enzyme for 1 h at 47 °C. The digested peptide was extracted by 0.2% formic acid, followed by 50% acetonitrile containing 0.2% formic acid and dried using speed vac. The peptide concentration was measured using Pierce™ Quantitative Colorimetric Peptide Assay (Thermo Scientific 23275). For fractionation, high pH STAGE fractionation of peptide or SDS-PAGE of protein was used. For SDS-PAGE, after top 12 protein depletion, the serum was boiled with 2× SDS-PAGE sample loading buffer (Invitrogen Cat# NP0007), then resolved on 10% Bis-Tris gel (Invitrogen Cat #NP0315BOX). The gel was stained by Coomassie blue and dissected into five slices for in gel digestion, as previously described [17]. For STAGE Tip fractionation, 10 μg of dried peptides were dissolved in 100 μl of pH 10 buffer (10 mM ammonium bicarbonate, pH 10, adjusted by NH_4OH) and subjected to a micro-pipette tip C18 column made from a 200-μl pipette tip by layering 2 mg of C18 matrix (Reprosil-Pur Basic C18, 3 μm, Dr. Maisch GmbH, Germany) on top of the C18 disk (3M, Empore™ C18) plug. The peptides were eluted with step gradient of 100 μl of 9%, 21%, and 35% acetonitrile (in pH 10 buffer) and pooled into 2 pools (9% with 35% eluent, and 21% eluent) and vacuum-dried for nano ultra high-performance liquid chromatography/tandem mass spectrometry (nano-HPLC-MS/MS). Dried peptides were dissolved in 20 μl of loading solution (5% methanol containing 0.1% formic acid) and subjected to nano-HPLC-MS/MS assay as described previously [18].

≡ Outline   📄 Download   Share   Export
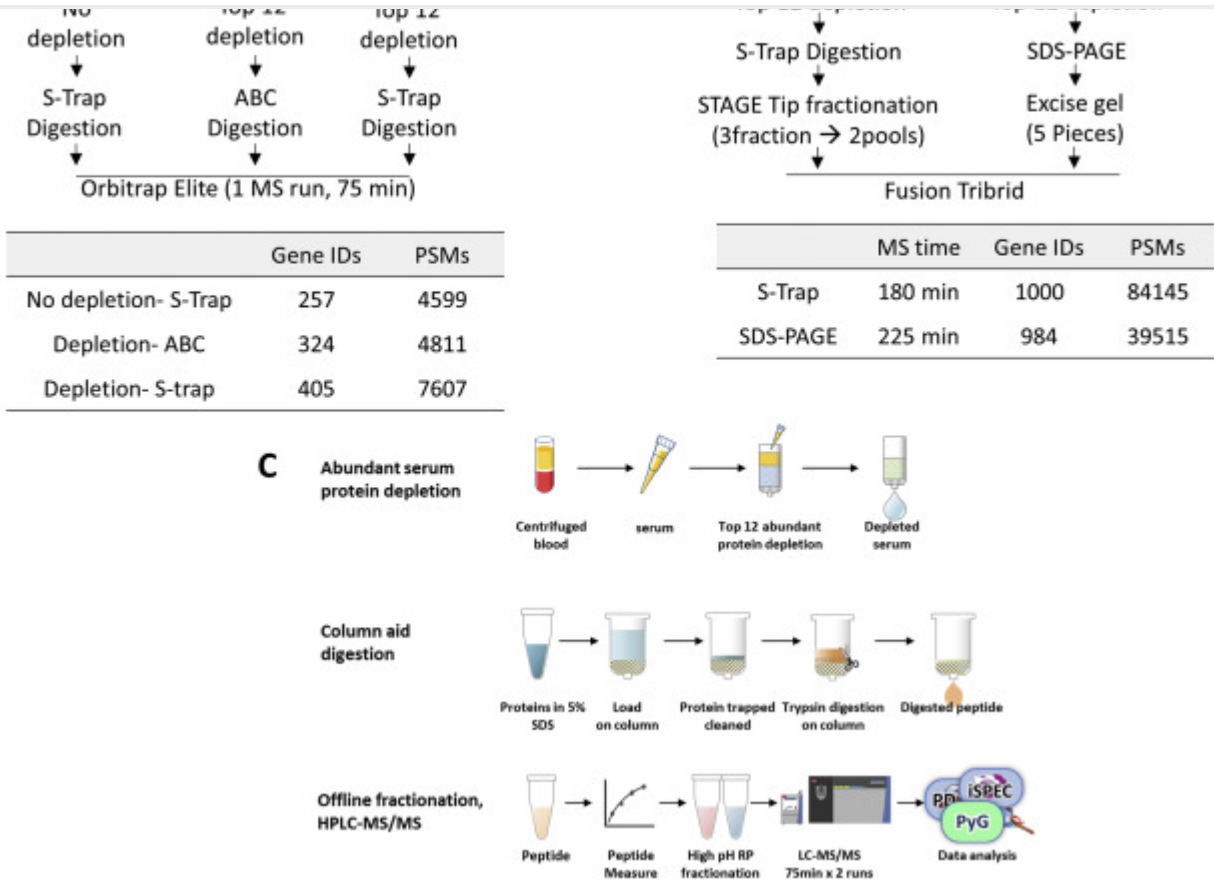
Download : Download high-res image (428KB)   Download : Download full-size image

Fig. 1. Test of different sample preparation methods. A. Comparison of the effect of Top 12 abundant protein depletion, direct in-solution digestion and S-Trap aid in column digestion method. B. Comparison of the fractionation method between high pH STAGE tip method and SDS-PAGE. Recovered protein (shown in Gene Protein Product, GPs) and Peptide Spectrum Matches (PSMs) numbers are representative results from triple repeat. C. Schematic illustration of established workflow in the serum profiling process. S-Trap aided trypsin digestion, high pH STAGE tip method for preparation of serum samples was used.

For Orbitrap Elite MS analysis, digested peptides were analyzed by a nano-HPLC 1000 system (Thermo Scientific) coupled to an Orbitrap Elite Hybrid mass spectrometer. An in-housed trap column packed with 1.9 μm Reprosil-Pur Basic C18 beads (2 cm × 100 μm) and an in-housed 5 cm × 150 μm capillary column packed with 1.9 μm Reprosil-Pur Basic C18 beads were used. A 75-min discontinuous gradient of 4–26% acetonitrile, 0.1% formic acid at a flow rate of 800 nl/min was applied to column then electro-sprayed into the mass spectrometer. The instrument was operated under the control of Xcalibur software version 2.2 (Thermo Fisher

resolution of 240,000. Collision-induced dissociation (CID) fragmented MS/MS spectrum was acquired in ion-trap with rapid scan mode.

For Fusion Lumos MS analysis, digested peptides were analyzed by a nano-HPLC 1200 system (Thermo Scientific) coupled to an Orbitrap Fusion™ Lumos™ Tribrid™ (Fusion Lumos, Thermo Scientific) mass spectrometer. An in-housed trap column packed with 3 μm Reprosil-Pur Basic C18 beads (2 cm × 100 μm) and an in-housed 5 cm × 150 μm capillary column packed with 1.9 μm Reprosil-Pur Basic C18 beads were used. A 90-min discontinuous gradient of 2–24% acetonitrile, 0.1% formic acid at a flow rate of 800 nl/min was applied to column then electro-sprayed into the mass spectrometer. The instrument was operated under the control of Xcalibur software version 4.1 (Thermo Fisher Scientific) in data-dependent mode, acquiring fragmentation spectra of the top 50 strongest ions. Parent MS spectrum was acquired in the Orbitrap with full MS range of 300–1400 m/z in the resolution of 120,000. Higher-energy collisional dissociation (HCD) fragmented MS/MS spectrum was acquired in ion-trap with rapid scan mode. The MS/MS spectra were searched against target-decoy Human RefSeq database (release 2015.06, containing 73,637 entries) in Proteome Discoverer 2.1 interface (Thermo Fisher) with Mascot algorithm (Mascot 2.4, Matrix Science). The precursor mass tolerance of 20 ppm and fragment mass tolerance of 0.5 Da was allowed. Two maximum missed cleavage, and dynamic modifications of acetylation of N-term and oxidation of methionine were allowed. Assigned peptides were filtered with a 1% false discovery rate (FDR) using Percolator validation based on q-value. The Peptide Spectrum Matches (PSMs) output from PD2.1 was used to group peptides onto gene level using 'gpGrouper' algorithm [19]. An in-housed program, gpGrouper, uses a universal peptide grouping logic to accurately allocate and provide MS1 based quantification across multiple gene products. Gene-protein products (GPs) quantification was performed using the label-free, intensity-based absolute quantification (iBAQ) approach and then normalized to FOT (a fraction of the total protein iBAQ amount per experiment). FOT was defined as an individual protein's iBAQ divided by the total iBAQ of all identified proteins within one experiment.

2.3.1. Statistical analysis

Statistical analysis of proteomics was done using Microsoft Excel Program. Paired two-tailed Student's t-test using log converted iFOT was used to determine statistically significantly regulated proteins from samples collected before 30-day intermittent fasting, at the end of 4th week during 30-day intermittent fasting and one week after 30-day intermittent fasting. Proteins that showed P < 0.05 and equal to or greater than 4-fold change were considered as significant. Volcano plot analysis was performed to display the GP levels that had an equal to or greater than 4-fold significant change at the end of 4th week during 30-day intermittent fasting and one week after 30-day intermittent fasting compared with the GP levels before 30-day intermittent fasting.

☰ Outline   📕 Download   Share   Export

diastolic blood pressures, mean arterial pressure, lipid profile (total cholesterol, triglyceride, high-density lipoprotein, low-density lipoprotein), insulin, glucose, homeostatic model assessment-insulin resistance (HOMA-IR) [20], homocysteine, C-reactive protein, interleukin 1b, interleukin 6, interleukin 8, tumor necrosis factor-alpha, leptin, and adiponectin were measured within four weeks before 30-day intermittent fasting, at the end of 4th week during 30-day intermittent fasting, and one week after completion of 30-day intermittent fasting.

2.4.1. Statistical analysis

Statistical analysis of clinical metabolic parameters and serum biomarkers performed using SAS Version 9.4 TS Level 1 M5 X64_10PRO platform (SAS, Cary, NC) [21]. Student's paired *t*-test was used to compare the levels of continuous variables measured at the end of 4th week during 30-day intermittent fasting, and one week after completion of 30-day intermittent fasting with the levels measured before 30-day intermittent fasting. A two-tailed *P* value of< 0.05 was considered statistically significant.

3. Fecal microbiota

The fecal microbiota of 70 fecal samples (14 subjects × 5 samples collected from each subject) was profiled for the analysis of samples obtained before 30-day intermittent fasting (before), at the 2nd and 4th week during 30-day intermittent fasting (during), and one week after 30-day intermittent fasting (after). The 16S rRNA gene sequencing methods were adapted from the methods developed for the Earth Microbiome Project [22,23] and NIH-Human Microbiome Project [24,25]. Fecal microbiota analysis is described in Supplementary materials.

4. Results

4.1. Subjects

Fourteen healthy subjects (13 males:1 female) with a mean age of 32 were enrolled in the study. All subjects fasted for over 14 h daily for 30 consecutive days beginning from May 16, 2018, until June 14, 2018, except for one subject who fasted for 26 days. The minimum required duration of daily fasting was 14 h, 23 min for the shortest day (May 16, 2018), and 14 h, 48 min for the longest day (June 14, 2018). All subjects tolerated intermittent fasting (no food or drink) well without any complications. The first blood collection occurred before the initiation of 30-day intermittent fasting. The second blood collection occurred on an average of 28 days after the initiation of 30-day intermittent fasting (at the end of the 4th week during 30-day intermittent fasting). The third blood collection occurred on an average of 8.5 days after the completion of 30-day intermittent fasting (one week after 30-day intermittent fasting).

proteome coverage. As shown in Fig. 1A, the top 12 abundant protein depletion provides around 58% proteome increase (257 vs. 405 GPs). Suspension traps (S-Trap) were recently reported as a sensitive and time-saving way of proteome profiling sample preparation [26]. Compared to direct in-solution digest, S-Trap provides a 25% better recovery in proteome coverage (324 vs. 405 GPs). Also, we tested two different ways of pre-sample fractionation before UPLC-MS/MS. Comparing high pH STAGE tip and SDS-PAGE, the STAGE tip provides deeper proteome coverage within shorter MS analysis time (Fig. 1B). So, we decided to use S-Trap aided trypsin digestion, high pH STAGE tip method for the preparation of fasting serum samples. The established workflow is shown in Fig. 1C.

Proteome coverage and its dynamic order of average iFOT values from the end of 4th week during 30-day intermittent fasting samples are shown in Fig. 2A. A total of 3181 GPs were recovered with over eight orders of magnitude of dynamic range. There was significant fold change in the levels of multiple GPs at the end of 4th week during 30-day intermittent fasting compared with the levels before 30-day intermittent fasting (Fig. 2B, Supplementary Table S1). Fig. 2A, B, and Table 1A display selected GPs of interest that are associated with immune system regulation, DNA repair, carcinogenesis, tumor suppression, circadian clock, Alzheimer's disease, and neuropsychiatric disorders. There was an average 40 fold increase in asialoglycoprotein receptor 2 (ASGR2) (log2 fold = 5.315, P = .0058), 45 fold increase in the centrosomal protein 164 (CEP164) (log2 fold = 5.499, P = .0157), 160 fold increase in complement factor H related 1 (CFHR1) (log2 fold = 7.320, P = .0199), 14 fold increase in collectin subfamily member 10 (COLEC10) (log2 fold = 3.781, P = .0383), 9 fold increase in large tumor suppressor kinase 1 (LATS1) (log2 = 3.243, P = .0415), 11 fold increase in NR1D1 nuclear receptor subfamily 1 group D member 1 (NR1D1) (log2 = 3.455, P = .0417), and 25 fold increase in homer scaffold protein 1 (HOMER1) (log2 fold = 4.664, P = .0443) GP levels at the end of 4th week during 30-day intermittent fasting compared with the levels before 30-day intermittent fasting. The amount of these GPs of interest was relatively high, located in the top 50% rank order (Fig. 2A). We found a significant reduction in the amyloid beta precursor protein (APP) (log2 fold = –7.147, P = .0026), beta-1,4-galactosyltransferase 1 (B4GALT1) (log2 fold = –3.194, P = .0192), ArfGAP with SH3 domain, ankyrin repeat and PH domain 1 (ASAP1) (log2 fold = –3.715, P = .0219), tankyrase 2 (TNKS2) (log2 fold = –3.416, P = .0402), flavin containing dimethylaniline monooxygenase 5 (FMO5) (log2 fold = –4.031, P = .0406), ribosome binding protein 1 (RRBP1) (log2 fold = –3.403, P = .0408), cAMP regulated phosphoprotein 21 (ARPP21) (log2 fold = –4.977, P = .0410) and HECT, UBA and WWE domain containing E3 ubiquitin protein ligase 1 (HUWE1) (log2 fold = –2.931, P = .0411) GP levels at the end of 4th week during 30-day intermittent fasting compared with the levels before 30-day intermittent fasting.

The proteome coverage and its dynamic order from triplicate of samples collected one week after 30-day intermittent fasting are shown in Fig. 2C. A total of 3416 GPs were recovered with over

intermittent fasting (Fig. 2D, Supplementary Table S2). Fig. 2C, D and Table 1B display selected GPs of interest that are associated with insulin signaling, cytoskeleton remodeling, glucose and lipid metabolism, carcinogenesis, Alzheimer's disease and neuropsychiatric disorders. There was an average 127-fold increase in the tropomyosin 3 (TPM3), (log2 fold = 6.988, P = .0007), 95-fold increase in profilin 1 (PFN1) (log2 fold = 6.566, P = .0060), 21-fold increase in cofilin 1 (CFL1) (log2 fold = 4.375, P = .0162), 13-fold increase in pyruvate kinase M1/2 (PKM) (log2 fold = 3.743, P = .0287), 32-fold increase in perilipin 4 (PLIN4) (log2 fold = 4.997, P = .0383), and 15-fold increase in tropomyosin 4 (TPM4) (log2 fold = 3.938, P = .0446) GP levels one week after 30-day intermittent fasting compared with the levels before 30-day intermittent fasting (Table 1B). The amount of these GPs was relatively high, rank order between 479 and 879 out of 3416 GPs (Fig. 2C). We found a significant reduction in the Rho guanine nucleotide exchange factor 28 (ARHGEF28) (log2 fold = −4.510, P = .0111), partner and localizer of BRCA2 (PALB2) (log2 fold = −3.715, P = .0147), SPARC related modular calcium binding 1 (SMOC1) (log2 fold = −4.776, P = .0264), spectrin repeat containing nuclear envelope protein 1 (SYNE1) (log2 fold = −2.576, P = .0274), interleukin 1 receptor associated kinase 3 (IRAK3) (log2 fold = −3.097, P = .0357), TNKS2 (log2 fold = −3.416, P = .0402), mucin 20, cell surface associated (MUC20) (log2 fold = −3.149, P = .0404), ARPP21 (log2 fold = −4.977, P = .0410) and HUWE1 (log2 fold = −2.931, P = .0411) GP levels one week after 30-day intermittent fasting compared with the levels before 30-day intermittent fasting.

Fig. 3 shows the change (logiFOT X 10^5) in the levels of 13 selected GPs that significantly increased at the end of 4th week during 30-day intermittent fasting or one week after 30-day intermittent fasting compared with the levels before 30-day intermittent fasting.

Download : Download high-res image (703KB)   Download : Download full-size image
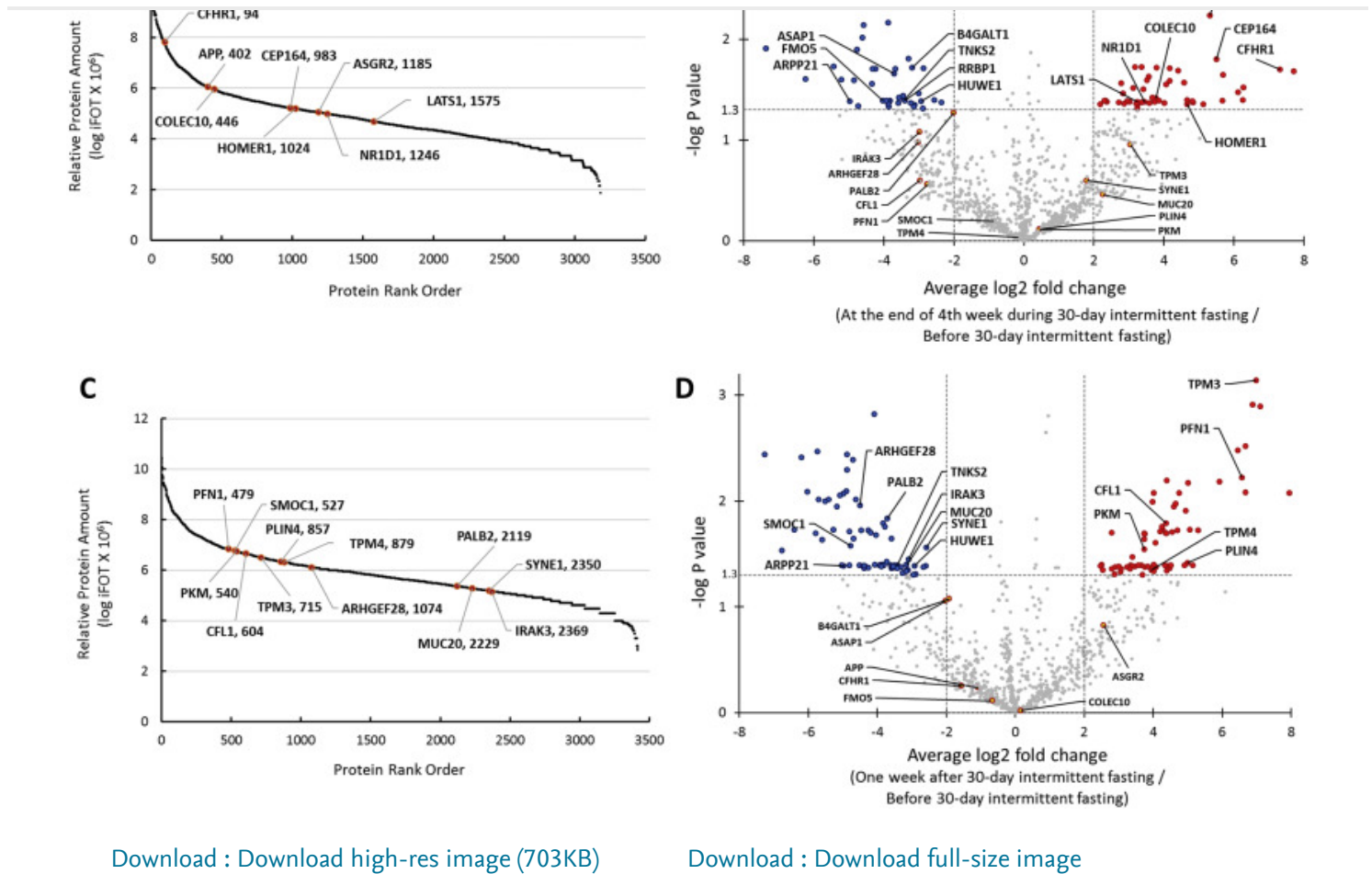
Fig. 2. A. Distribution of normalized relative gene protein product (GP) amount and location of significantly changed selected proteins in serum samples taken at the end of 4th week during 30-day intermittent fasting shown in GP name and rank order. B. Volcano plot shows GPs that had an equal to or >4-fold significant change (blue and red colors represent a significant decrease and increase in the levels of GPs, respectively) at the end of 4th week during 30-day intermittent fasting compared with the levels before 30-day intermittent fasting. C. Distribution of normalized relative GP amount and location of significantly changed selected proteins in serum samples taken one week after 30-day intermittent fasting shown in GP name and rank order. D. Volcano plot shows GPs that had an equal to or >4-fold significant change (blue and red colors represent a significant decrease and increase in the levels of GPs, respectively) one week after 30-day intermittent fasting compared with the levels before 30-day intermittent fasting. (For interpretation of the references to colour in this figure legend, the reader is referred to the web version of this article.)

A. Selected Gene Protein Products (GP)s that Are Significantly Up- or Downregulated at the End of 4th Week During 30-Day Intermittent Fasting Compared with Baseline (Before 30-Day Intermittent Fasting)

Upregulated Gene Symbol	Upregulated Gene Name	Upregulated Gene ID	Average Log2 Fold Change	Paired P Value
ASGR2	asialoglycoprotein receptor 2	433	5.315	0.0058
CEP164	centrosomal protein 164	22897	5.499	0.0157
CFHR1	complement factor H related 1	3078	7.320	0.0199
COLEC10	collectin subfamily member 10	10584	3.781	0.0383
LATS1	large tumor suppressor kinase 1	9113	3.243	0.0415
NR1D1	nuclear receptor subfamily 1 group D member 1	9572	3.455	0.0417
HOMER1	homer scaffold protein 1	9456	4.664	0.0443

Downregulated Gene Symbol	Downregulated Gene Name	Downregulated Gene ID	Average Log2 Fold Change	Paired P-Value
APP	amyloid beta precursor protein	351	-7.147	0.0026
B4GALT1	beta-1,4-galactosyltransferase 1	2683	-3.194	0.0192
ASAP1	ArfGAP with SH3 domain, ankyrin repeat and PH domain 1	50807	-3.715	0.0219
TNKS2	tankyrase 2	80351	-3.416	0.0402
FMO5	flavin containing dimethylaniline monoxygenase 5	2330	-4.031	0.0406
RRBP1	ribosome binding protein 1	6238	-3.403	0.0408
ARPP21	cAMP regulated phosphoprotein 21	10777	-4.977	0.0410
HUWE1	HECT, UBA and WWE domain containing E3 ubiquitin protein ligase 1	10075	-2.931	0.0411

Outline   Download   Share   Export

Upregulated Gene Symbol	Upregulated Gene Name	Upregulated Gene ID	Average Log2 Fold Change	Paired P Value
TPM3	tropomyosin 3	7170	6.988	0.0007
PFN1	profilin 1	5216	6.566	0.0060
CFL1	cofilin 1	1072	4.375	0.0162
PKM	pyruvate kinase M1/2	5315	3.743	0.0287
PLIN4	perilipin 4	729359	4.997	0.0383
TPM4	tropomyosin 4	7171	3.938	0.0446

Downregulated Gene Symbol	Downregulated Gene Name	Downregulated Gene ID	Average Log2 Fold Change	Paired P-Value
ARHGEF28	Rho guanine nucleotide exchange factor 28	64283	-4.510	0.0111
PALB2	partner and localizer of BRCA2	79728	-3.715	0.0147
SMOC1	SPARC related modular calcium binding 1	64093	-4.776	0.0264
SYNE1	spectrin repeat containing nuclear envelope protein 1	23345	-2.576	0.0274
IRAK3	interleukin 1 receptor associated kinase 3	11213	-3.097	0.0357
TNKS2	tankyrase 2	80351	-3.416	0.0402
MUC20	mucin 20, cell surface associated	200958	-3.149	0.0404
ARPP21	cAMP regulated phosphoprotein 21	10777	-4.977	0.0410
HUWE1	HECT, UBA and WWE domain containing E3 ubiquitin protein ligase 1	10075	-2.931	0.0411

Outline   Download   Share   Export

Outline   Download   Share   Export
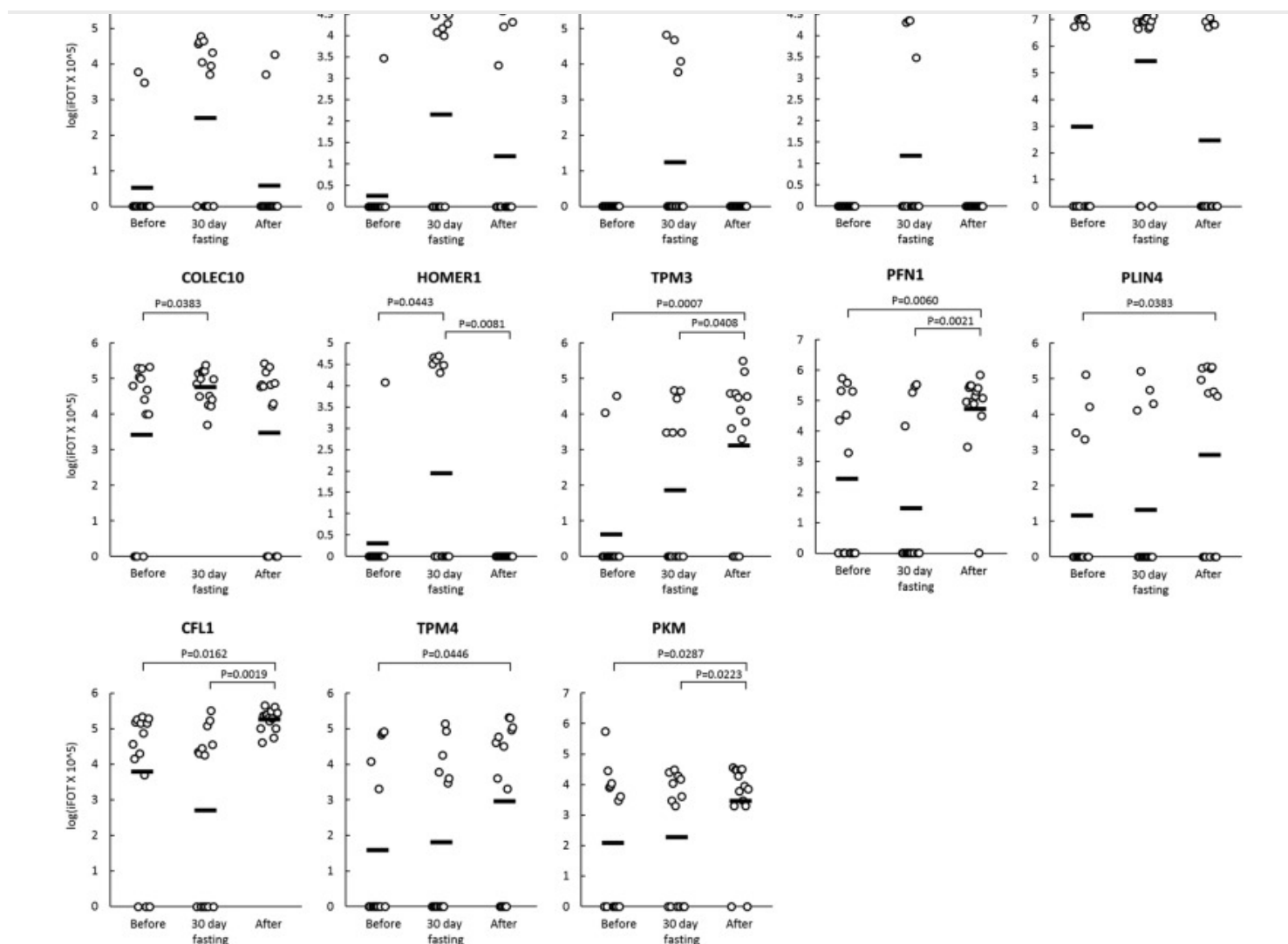
Download : Download high-res image (289KB)   Download : Download full-size image

Fig. 3. Change (logiFOT X 10^5) in the levels of 13 selected GPs that significantly increased at the end of 4th week during 30-day intermittent fasting (30-day fasting) or one week after 30-day intermittent fasting (After) compared with the levels before 30-day intermittent fasting (Before).

Fig. 4 shows the change (logiFOT X 10^5) in the levels of 14 selected GPs that significantly decreased at the end of 4th week during 30-day intermittent fasting or one week after 30-day intermittent fasting or both at the end of 4th week during 30-day intermittent fasting and one week after 30-day intermittent fasting compared with the levels before 30-day intermittent fasting.
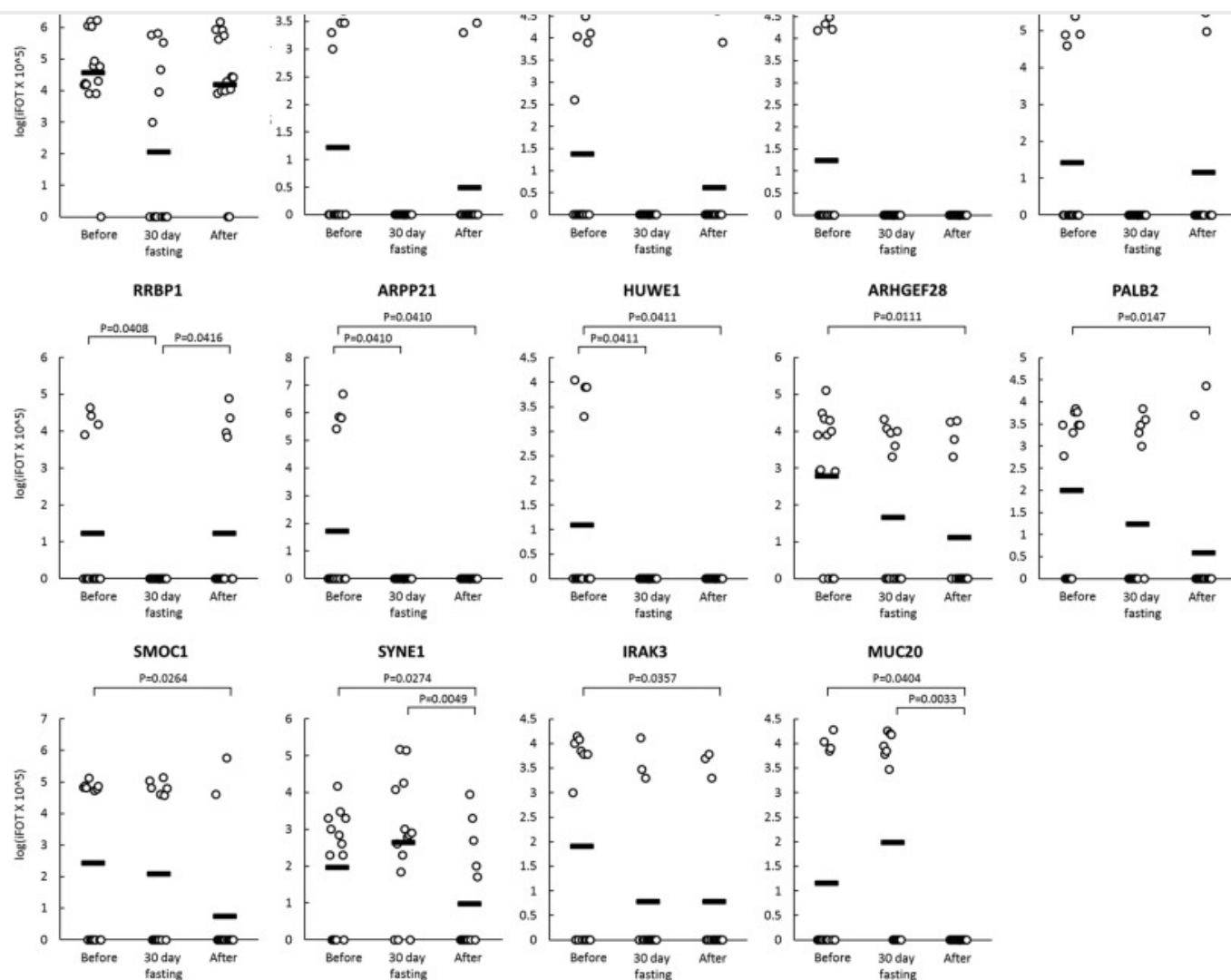
Download : Download high-res image (302KB)   Download : Download full-size image

Fig. 4. Change (logiFOT X 10^5) in the levels of 14 selected GPs that significantly decreased at the end of 4th week during 30-day intermittent fasting (30-day fasting) or one week after 30-day intermittent fasting (After) or both at the end of 4th week during 30-day intermittent fasting and one week after 30-day intermittent fasting compared with the levels before 30-day intermittent fasting (Before).

4.3. Conventional metabolic parameters and serum biomarkers

Overall, there was no significant change in clinical metabolic parameters and serum metabolic biomarkers at the end of 4th week during 30-day intermittent fasting and one week after 30-day

4.4. Fecal microbiota

Although increased alpha diversity richness was present among the subjects, no significant statistical differences were observed in richness and diversity (Shannon and Simpson's) when comparing the collection periods (Supplementary Fig. S4A). Thus, bacterial richness and diversity did not change significantly over the three collection periods. Similarly, the beta-diversity analysis using Weighted and Unweighted UniFrac distance metrics did not reveal differences in the microbial structure between the three periods (Supplementary Fig. S4B). Overall, the grouped subjects from the three periods shared two dominant orders among the abundant taxa: Clostridiales (Firmicutes) and Bacteroidales (Bacteroidetes) (Supplementary Fig. S4C). Further results of fecal microbiota analysis are included in Supplementary Materials.

5. Discussion

Herein, we conducted the first human study of serum proteomics of 30-day dawn to sunset intermittent fasting with simultaneous assessment of clinical metabolic parameters, multiple serum biomarkers, and fecal microbiota in 14 healthy subjects. Our study has important clinical implications: Our results showed that intermittent fasting from dawn to sunset for over 14 h daily for 30 consecutive days was associated with an anticancer serum proteomic signature, upregulated the key regulatory proteins of glucose and lipid metabolism, insulin signaling, circadian clock, DNA repair, cytoskeleton remodeling, immune system and cognitive function, and resulted in a serum proteome protective against cancer, metabolic syndrome, inflammation, Alzheimer's disease, and several neuropsychiatric disorders. Importantly, these findings occurred in the absence of any calorie restriction and significant weight loss. We assessed changes in the serum proteome, serum biomarkers, fecal microbiome, and clinical parameters not only at the end of 4th week during 30-day intermittent fasting but also one week after completion of 30-day intermittent fasting. To our knowledge, this is also the first study where compliance with fasting was monitored with objective measures (13C-isotopic breath enrichment test) rather than relying on study participants' self-reporting.

5.1. Intermittent fasting from dawn to sunset is associated with anticancer proteomic signature

We found a significant increase in the levels of specific proteins that are downregulated in several cancers, and therefore associated with metastasis and poor prognosis, at the end of 4th week during 30-day intermittent fasting. LATS1 is a large tumor suppressor kinase 1 that was shown to suppress proliferation, progression, and invasion of several tumors [27], e.g. hepatocellular carcinoma [28], cervical cancer [29], and non-small cell lung cancer [30]. A genomic mapping using data collected from the Catalogue of Somatic Mutations in Cancer (COSMIC) and

intermittent fasting compared with the level before 30-day intermittent fasting.

CFHR1 (also known as CFHL1) and COLECT10 are abundantly expressed in the liver [27]. CFHR1 and COLEC10 were shown to be downregulated in hepatocellular carcinoma and associated with poor prognosis [32,33]. We found an average 160 and 14 fold increase in the CFHR1 and COLEC10 GP levels, respectively, at the end of 4th week during 30-day intermittent fasting compared with the levels before 30-day intermittent fasting.

We also found a significant reduction in the levels of specific proteins that are overexpressed in several cancers, and therefore associated with metastasis and poor prognosis, at the end of 4th week during 30-day intermittent fasting or one week after 30-day intermittent fasting.

B4GALT1 is overexpressed in several tumors, including hepatocellular carcinoma [34], lung cancer [35], and breast cancer [36]. Inhibition of B4GALT1 was shown to remove multidrug resistance in leukemia, which can potentially increase sensitivity to chemotherapy. [37] We found a significant reduction in the B4GALT1 GP level at the end of 4th week during 30-day intermittent fasting compared with the level before 30-day intermittent fasting.

ASAP1 overexpression was reported in laryngeal squamous cell carcinoma [38] and epithelial ovarian cancer [39]. We found a significant reduction in the ASAP1 GP level at the end of 4th week during 30-day intermittent fasting compared with the level before 30-day intermittent fasting.

FMO5 is a flavin-containing dimethylaniline monooxygenase that has a biased expression in the liver [27]. Overexpression of FMO5 was shown to be a poor prognostic indicator in colorectal cancer [40]. We found a significant reduction in the FMO5 GP level at the end of 4th week during 30-day intermittent fasting compared with the level before 30-day intermittent fasting.

RRBP1 was shown to be overexpressed in colorectal cancer [41] and endometrial endometrioid adenocarcinoma [42]. We found a significant reduction in the RRBP1 GP level at the end of 4th week of intermittent fasting compared with the level before 30-day intermittent fasting.

TNKS2 (also known as TANK2 and TNKL), which is a TTAGGG repeat binding factor 1 (TRF1) [43]-associated poly(ADP-ribose) polymerase was shown to induce rapid necrotic cell death [44]. A potential association between TNKS2 and cancer was reported [45]. Overexpression of TNKS2 was found in breast cancer [46]. We found a significant reduction in the TNKS2 GP level at the end of 4th week during and one week after 30-day intermittent fasting compared with the level before 30-day intermittent fasting.

HUWE1, an E3 ubiquitin protein ligase, ubiquitinates the tumor suppressor p53 leading to its degradation. [27] The inactivation or deletion of HUWE1 upregulates p53 and thereby inhibits the development and proliferation of non-small lung cancer [47]. HUWE1 overexpression was

week after 30-day intermittent fasting compared with the level before 30-day intermittent fasting.

ARHGEF28, also known as RGNEF, was shown to play a key role in tumor progression and invasion in colon cancer via focal adhesion kinase (FAK) [49]. We observed a significant reduction in the ARHGEF28 GP level one week after 30-day intermittent fasting compared with the level before 30-day intermittent fasting.

Pathogenic variants of the PALB2 gene was implicated as a risk factor in the development of bilateral breast cancer [50]. We found a significant reduction in the PALB2 GP level one week after 30-day intermittent fasting compared with the level before 30-day intermittent fasting.

SMOC1 that has a biased expression in the brain [27] was found to be overexpressed in brain tumors including oligodendrogliomas, glioblastomas and astrocytomas compared with control brain tissues [51]. We found a significant reduction in SMOC1 GP level one week after 30-day intermittent fasting compared with the level before 4-week intermittent fasting.

The role of interleukin 1 receptor-associated kinase (IRAK) signaling in tumor development and progression is well-defined. [52] IRAK3 (also known as IRKM) deficient mice were shown to be protected against tumor development. [53] We found a significant reduction in IRAK3 GP level one week after 30-day intermittent fasting compared with the level before 30-day intermittent fasting.

Overexpression of MUC20 was reported in colorectal, endometrial and ovarian cancers as a predictor of tumor progression and aggressiveness. [54] [55] [56] We found a significant reduction in the MUC20 GP level one week after 30-day intermittent fasting compared with the level before 30-day intermittent fasting.

Altogether, our findings showed that 30-day dawn to sunset intermittent fasting resulted in an anticancer serum proteome in healthy subjects. Our results suggest that 30-day intermittent fasting can be a preventive and adjunct treatment in several cancers and increase sensitivity to chemotherapy.

5.2. Intermittent fasting from dawn to sunset upregulates expression of CEP164, a key DNA repair protein

CEP164 gene plays a primary role in the development and function of the primary cilium [27]. It is also a mediator protein in the ultraviolet and ionizing radiation-induced DNA damage repair signaling pathway [57] and recruited to DNA sites damaged by ultraviolet [58]. We found an average 45 fold increase in the CEP164 GP level at the end of 4th week during 30-day intermittent fasting compared with the level before 30-day intermittent fasting. These findings suggest that

5.3. Intermittent fasting from dawn to sunset upregulates expression of NR1D1, a circadian clock protein

NR1D1 (also known as REV-ERBα), a component of the circadian clock, regulates the expression of genes involved in metabolism and inflammation [27]. A murine study demonstrated that NR1D1 plays a critical role in the prevention of metabolic syndrome; the deletion of REV-ERBα (NR1D1) resulted in lipoprotein lipase overexpression in peripheral tissues, increased fat storage in the liver and adipose tissues, and susceptibility to obesity induced by a high-fat diet [59]. Pharmacologic NR1D1 activation was shown to reduce the severity of acute peritonitis and prevent fulminant hepatitis by inhibiting the NLRP3 inflammasome pathway. [60] We observed an average 11 fold increase in the NR1D1 GP level at the end of 4th week during 30-day intermittent fasting compared with the level before 30-day intermittent fasting. These findings suggest that dawn to sunset 30-day intermittent fasting can reduce fat accumulation in the liver and adipose tissues, and attenuates NLRP3-driven inflammation, therefore it can be an adjunct treatment of patients with metabolic syndrome and nonalcoholic fatty liver disease.

5.4. Intermittent fasting from dawn to sunset upregulates expression of ASGR2, a subunit of asialogylcoprotein receptor which is a key hepatic immunoregulatory protein

ASGR2 gene encodes for one of the subunits of the asialoglycoprotein receptor and abundantly expressed in the liver [27]. The asialoglycoprotein receptor plays a vital role in the clearance of apoptotic cell debris and immune regulation in the liver [61,62]. Apoptosis, which is programmed cell death, is a fundamental mechanism to prevent inflammation, fibrosis, and liver cancer [61]. In several chronic liver diseases, cirrhosis, and hepatocellular carcinoma, there is a reduction in the surface distribution of ASGPRs and ASGPR mRNA expression [63,64], and this can result in dysregulation of apoptosis, and inefficient clearance of apoptotic cell debris leading to chronic inflammation, and breakdown of self-tolerance [[61], [62], [63], [64]]. We observed an average 40 fold increase in the ASGR2 GP level at the end of 4th week of intermittent fasting compared with the level before 30-day intermittent fasting. Altogether, these findings suggest that 30-day intermittent fasting from dawn to sunset can enhance the hepatic clearance of apoptotic cell debris, reduce inflammation, and optimize immune function.

5.5. Intermittent fasting from dawn to sunset results in a serum proteome protective against cognitive dysfunction, Alzheimer's disease and several neuropsychiatric diseases

HOMER1 gene is abundantly expressed in the brain [27]. Alterations in HOMER1 levels in the hippocampus and cingulate gyrus were reported in schizophrenia, major depression, and bipolar

addiction [66]. HOMER1 knockout mice were shown to have neurochemical and behavioral abnormalities similar to the abnormalities observed in schizophrenia. [67] Amyloid precursor protein and presenilin 1 transgenic mice as an Alzheimer's disease model was shown to have reduced HOMER1 mRNA expression [68]. In addition to these reports, HOMER1 expression was found to be increased in the hippocampus post-synaptic densities of Long Evans aged rats with unimpaired memory compared with those with impaired memory [69]. We found an average 25 fold increase in the HOMER1 GP level at the end of 4th week during 30-intermittent fasting compared with the level before 30-day intermittent fasting.

APP, the precursor of amyloid β, appears to play a significant role in the development of Alzheimer's disease [27]. APP was proposed to trigger atherothrombosis after the accumulation of amyloid β peptides in the cerebral vessels in Alzheimer's disease [70]. We observed a significant reduction in the APP GP level at the end of 4th week during 30-day intermittent fasting compared with the level before 30-day intermittent fasting.

ARPP-21 that is abundantly expressed in the brain, is another gene that plays a significant role in the development of Alzheimer's disease [27]. A genome-wide study conducted among subjects with Alzheimer's disease showed a single-nucleotide polymorphism (SNP) located proximal to the ARPP-21 gene. [71] We found a significant reduction in the ARPP21 GP level at the end of 4th week during and one week after 30-day intermittent fasting compared with the level before 30-day intermittent fasting.

According to a genome-wide study conducted among 1527 patients with bipolar disorders (1579 controls) and 1159 patients with recurrent unipolar depression (2592 controls), a SNP located in the SYNE1 gene was significantly associated with the risk of bipolar depression and recurrent major depression. [72] We found a significant reduction in the SYNE1 GP level one week after 30-day intermittent fasting compared with the level before 30-day intermittent fasting.

Altogether, these findings suggest that 30-day dawn to sunset intermittent fasting can have implications in the improvement of cognitive function, prevention, and treatment of Alzheimer's disease and several neuropsychiatric disorders, including major depression, bipolar disorder, and schizophrenia.

5.6. Intermittent fasting from dawn to sunset upregulates expression of key regulatory proteins of glucose and lipid metabolism, insulin signaling, actin cytoskeleton remodeling

We found significant upregulation of several signature genes that play a key role in cytoskeleton remodeling, glucose, and lipid metabolism, and blood pressure regulation one week after completion of 30-day intermittent fasting. There was an average 127-fold increase in the TPM3

that are well known for their role in skeletal and cardiac muscle contraction [73,74]. They are also components of the actin cytoskeleton in non-muscle cells and play a key role in stabilization, regulation, and remodeling of the actin cytoskeleton. [[73], [74], [75]] The actin cytoskeleton is thought to orchestrate cell division, proliferation, support, movement, intra- and intercellular communications, and specifically, organelle trafficking [76]. Dysfunction of the actin cytoskeleton has been shown to result in impaired exocytosis of glucose transporter (GLUT4) and thereby in insulin resistance [[77], [78], [79]]. TPM3 gene encodes for tropomyosin 3.1 that plays a crucial role in remodeling insulin-induced actin cytoskeleton, thereby increasing insulin sensitivity, and protecting against high-fat diet [77]. Similar to TPM3, the TPM4 gene encodes for a protein that binds cytoskeletal actin [27] that plays a key role in insulin responsiveness.

Tropomyosins play a vital role not only in glucose regulation but also in blood pressure regulation by stabilizing and remodeling the actin cytoskeleton [80]. Polymorphisms in TPM3 gene expression in erythrocytes and leukocytes may result in dysfunctional TPMN protein, and thereby, it can lead to essential hypertension [80]. Earlier reports of dawn to sunset fasting showed that there was a significant reduction in systolic blood pressure and pulse-pressure at the end of fourth week of dawn-to-sunset fasting compared with pressures measured before fasting. [81,82]

In addition to the upregulation of TPM3 and TPM4, there was an average 95 fold increase in the PFN1 GP level one week after 30-day intermittent fasting compared with the level before fasting. PFN1 encodes for cytoskeleton proteins that are involved in actin dynamics [27]. It mediates communication between the cytoskeleton and cell membrane [83] and regulates migration, invasion, and morphogenesis of endothelial cells [84].

Our results also showed that 30-day intermittent fasting upregulated PLIN4 GP. PLIN4 (also known as S3–12) has a biased expression in fat tissues [27]. A study conducted in Zucker rats showed that S3–12 (PLIN4) was downregulated in obese rats compared with lean ones, the peroxisome proliferator-activated receptor-γ (PPAR- γ) was the key regulator of PLIN4 expression in adipocytes, and activation of PPAR-γ resulted in upregulation of PLIN4 [85]. PPAR- γ activation improves insulin resistance and lipid metabolism [86]. Upregulation of PLIN4 expression one week after 30-day intermittent fasting suggests that 30-day intermittent fasting from dawn to sunset mimics PPAR-γ activators (e.g., pioglitazone), and this may be one of the mechanisms of intermittent fasting to improve insulin resistance and protect against adipose tissue dysfunction.

Another GP that was upregulated one week after 30-day intermittent fasting was CFL1. It has been shown that CFL1 plays a critical role in insulin-induced GLUT4 translocation, thereby glucose uptake [87]. We found an average 21 fold increase in the CFL1 GP level one week after 30-day intermittent fasting compared with the level before 30-day intermittent fasting, suggestive of

☰ Outline   📄 Download   Share   Export

There was an average 13 fold increase in the PKM GP level one week after 30-day intermittent fasting compared to the level before 30-day intermittent fasting. PKM encodes pyruvate kinase enzyme that is one of the key enzymes of glycolysis [27]. The upregulation of PKM2 in diabetes was shown to protect against the progression of diabetic nephropathy and mitochondrial dysfunction by reducing the production of toxic glucose metabolites [88].

In contrast to serum proteome, we found no significant change in the levels of conventional clinical metabolic parameters and serum metabolic biomarkers. This could be related to the fact that our study subjects were healthy, and therefore significant change in the levels of clinical metabolic parameters and serum metabolic biomarkers that would be otherwise expected in non-healthy subjects did not occur at the end of 30-day intermittent fasting compared with the levels before 30-day intermittent fasting.

Upregulation of TPM3, TPM4, PLIN4, CFL1, and PKM GP expression suggests that 30-day intermittent fasting can play a significant role in the prevention and treatment of metabolic syndrome. Metabolic syndrome is associated with insulin resistance, lipotoxicity, and inflammation [89]. It is also a significant risk factor for atherosclerotic cardiovascular disease and nonalcoholic fatty liver disease that can result in cirrhosis and hepatocellular carcinoma [89,90]. As such, the prevention of metabolic syndrome is a major public health concern, and better understandings are needed to guide effective interventions. The current daily dietary habit of many people is to eat periodically throughout the day into the evening, such that their bodies predominantly remain in the fed state. It is well known that nutrient utilization and body store utilization is influenced by macronutrient intake and meal timing [91,92]. It appears that intermittent fasting from dawn to sunset could offer a new therapeutic approach in metabolic syndrome and its complications.

Our proteomics study of intermittent fasting has several distinct features in terms of design and findings compared with the proteomics study conducted in healthy subjects by Harney et al. [93]. First and foremost, the study conducted by Harney et al. [93] did not assess the effect of strict intermittent fasting but rather the effect of a diet allowing the subjects to eat energy-free foods and low-energy broth and drink water, coffee, and tea during their fasting period that was scheduled for three nonconsecutive days of the week. In contrast, our study subjects fasted from dawn to sunset without eating or drinking for over 14 h daily for 30 consecutive days. This type of rhythmic consecutive intermittent fasting from dawn to sunset is compliant with circadian rhythm because daily fast starts at dawn (the first transition zone of the day) and ends at sunset (the second transition zone of the day) without any calorie restriction. Second, our subjects were not allowed to drink water during fasting; this ensured a complete lack of stimulus to the digestive system minimizing metabolic activities. Third, our study subjects did not have calorie restriction. Fourth, our results were distinct, showing an anticancer proteomic signature and

≣ **Outline**   📄 **Download**   **Share**   **Export**

~~and cognitive function associated with 30-day intermittent fasting.~~

Our study had limitations. Although we tested the effect of 30-day intermittent fasting, our study did not assess the impact of shorter duration of intermittent fasting (e.g., one or two weeks) or include a parallel control group of healthy subjects who did not fast for 30 days. A future study of 30-day intermittent fasting needs to be conducted in healthy subjects for external validation of the selected GPs discovered in our study.

6. Conclusions

In summary, our results suggest that 30-day intermittent fasting from dawn to sunset can be a preventive and therapeutic approach in cancer as well as in several metabolic, inflammatory and immune diseases, Alzheimer's disease and neuropsychiatric disorders by resulting in a proteome protective against carcinogenesis, obesity, diabetes, metabolic syndrome, inflammation, cognitive dysfunction, and mental health. Further studies are needed to test the effect of dawn to sunset intermittent fasting in larger cohorts with consideration given to shorter durations of fasting and longer longitudinal follow-up after completion of intermittent fasting.

The following are the supplementary data related to this article.

📄 Download : **Download Word document (64KB)**

Supplementary Table S1. Gene protein products (GP)s that are up- or downregulated at the end of 4th week during 30-day intermittent fasting (V2) compared with baseline (V1) (before 30-day intermittent fasting).

📄 Download : **Download Word document (58KB)**

Supplementary Table S2. Gene protein products (GP)s that are up- or downregulated one week after 30-day intermittent fasting (V3) compared with baseline (V1) (before 30-day intermittent fasting).

📄 Download : **Download Word document (16KB)**

:≡ **Outline**   📄 **Download**   **Share**   **Export**

intermittent fasting compared with the levels before 30-day intermittent fasting.

📄 Download : **Download Word document (880KB)**

Supplementary material

Meeting materials

1. Mindikoglu AL, Abdulsada MM, Jain A, Jung SY, Jalal PK, Opekun AR. Dawn to Sunset Fasting for 30 Days Induces Tropomyosin 1, 3 and 4 Genes in Healthy Volunteers: Its Clinical Implications in Metabolic Syndrome and Non-Alcoholic Fatty Liver Disease. Gastroenterology 2019, Vol. 156, Issue 6, S-1509–S-1510. Late-Breaking abstract was selected for a lecture presentation on May 21, 2019 at Digestive Disease Week (DDW) 2019, San Diego, CA. Control ID: 3194352.

2. Jain A, Jung SY, Abdulsada M, Opekun A, Malovannaya A, Jalal P, Mindikoglu AL. Dawn to Sunset Fasting for Four Weeks Has A Unique Proteomic Signature in Healthy Subjects. Abstract was selected for poster presentation on June 4, 2019 at ASMS Conference on Mass Spectrometry and Allied Topics, Atlanta, Georgia. Abstract ID number: 297726.

Funding

≡ **Outline**   📕 **Download**   **Share**   **Export**

Recommended articles   Citing articles (0)

References

[1]   M.W. Greene
       Circadian rhythms and tumor growth
       Cancer Lett., 318 (2) (2012), pp. 115-123
       Article   📕 Download PDF   View Record in Scopus   Google Scholar

[2]   A. Shetty, *et al.*
       Role of the circadian clock in the metabolic syndrome and nonalcoholic fatty liver disease
       Dig. Dis. Sci., 63 (12) (2018), pp. 3187-3206
       CrossRef   View Record in Scopus   Google Scholar

[3]   M. Hatori, *et al.*
       Time-restricted feeding without reducing caloric intake prevents metabolic diseases in mice fed a high-fat diet
       Cell Metab., 15 (6) (2012), pp. 848-860
       Article   📕 Download PDF   View Record in Scopus   Google Scholar

[4]   X.-M. Li, *et al.*
       Cancer inhibition through circadian reprogramming of tumor transcriptome with meal timing
       Cancer Res., 70 (8) (2010), pp. 3351-3360
       CrossRef   View Record in Scopus   Google Scholar

[5]   F. Damiola, *et al.*
       Restricted feeding uncouples circadian oscillators in peripheral tissues from the central pacemaker in the suprachiasmatic nucleus
       Genes Dev., 14 (23) (2000), pp. 2950-2961
       CrossRef   View Record in Scopus   Google Scholar

[6]   J.A. Evans
       Collective timekeeping among cells of the master circadian clock
       J. Endocrinol., 230 (1) (2016), pp. R27-R49
       View Record in Scopus   Google Scholar

[7]   R. Hara, *et al.*

Genes Cells, 6 (5) (2001), pp. 269-278

View Record in Scopus   Google Scholar

[8]   S.M. Reppert, D.R. Weaver

Coordination of circadian timing in mammals

Nature, 418 (6901) (2002), pp. 935-941

View Record in Scopus   Google Scholar

[9]   Y. Satoh, *et al.*

Time-restricted feeding entrains daily rhythms of energy metabolism in mice

Am. J. Phys. Regul. Integr. Comp. Phys., 290 (5) (2006), pp. R1276-R1283

CrossRef   View Record in Scopus   Google Scholar

[10]   K.A. Stokkan, *et al.*

Entrainment of the circadian clock in the liver by feeding

Science, 291 (5503) (2001), pp. 490-493

View Record in Scopus   Google Scholar

[11]   S. Yamazaki, *et al.*

Resetting central and peripheral circadian oscillators in transgenic rats

Science, 288 (5466) (2000), pp. 682-685

CrossRef   View Record in Scopus   Google Scholar

[12]   C. Dibner, U. Schibler, U. Albrecht

The mammalian circadian timing system: organization and coordination of central and peripheral clocks

Annu. Rev. Physiol., 72 (2010), pp. 517-549

CrossRef   View Record in Scopus   Google Scholar

[13]   A.L. Mindikoglu, *et al.*

Impact of time-restricted feeding and dawn-to-sunset fasting on circadian rhythm, obesity, metabolic syndrome, and nonalcoholic fatty liver disease

Gastroenterol. Res. Pract., 2017 (2017), p. 3932491

Google Scholar

[14]   H. Sherman, *et al.*

Long-term restricted feeding alters circadian expression and reduces the level of inflammatory and disease markers

J. Cell. Mol. Med., 15 (12) (2011), pp. 2745-2759

CrossRef   View Record in Scopus   Google Scholar

≔ **Outline**   📄 **Download**   **Share**   **Export**

~~TASED J., 26 (8) (2012), pp. 3493-3502~~

CrossRef   View Record in Scopus   Google Scholar

[16]   A.R. Opekun, A.M. Balesh, H.T. Shelby
Use of the biphasic (13)C-sucrose/glucose breath test to assess sucrose maldigestion in adults with functional bowel disorders
Biomed. Res. Int., 2016 (2016), p. 7952891
Google Scholar

[17]   S.Y. Jung, *et al.*
Proteomic analysis of steady-state nuclear hormone receptor coactivator complexes
Mol. Endocrinol., 19 (10) (2005), pp. 2451-2465
CrossRef   View Record in Scopus   Google Scholar

[18]   S.Y. Jung, *et al.*
An anatomically resolved mouse brain proteome reveals Parkinson disease-relevant pathways
Mol. Cell. Proteomics, 16 (4) (2017), pp. 581-593
CrossRef   View Record in Scopus   Google Scholar

[19]   A.B. Saltzman, *et al.*
gpGrouper: a peptide grouping algorithm for gene-centric inference and quantitation of bottom-up proteomics data
Mol. Cell. Proteomics, 17 (11) (2018), pp. 2270-2283
CrossRef   View Record in Scopus   Google Scholar

[20]   D.R. Matthews, *et al.*
Homeostasis model assessment: insulin resistance and β-cell function from fasting plasma glucose and insulin concentrations in man
Diabetologia, 28 (7) (1985), pp. 412-419
View Record in Scopus   Google Scholar

[21]   SAS software
Http://www.Sas.Com/. The data analysis for this paper was generated using SAS software, Version 9.4 of the SAS System for Windows
Copyright © 2016 SAS Institute Inc. SAS and all other SAS Institute Inc. product or service names are registered trademarks or trademarks of SAS Institute Inc, Cary, NC, USA (2016)
Google Scholar

[22]   J.G. Caporaso, *et al.*

☰ Outline　　📄 Download　　Share　　Export

Isme J., 6 (2012), p. 1621

CrossRef　　View Record in Scopus　　Google Scholar

[23]　J.G. Caporaso, *et al.*
Global patterns of 16S rRNA diversity at a depth of millions of sequences per sample
Proc. Natl. Acad. Sci. U. S. A., 108 (Suppl. 1) (2011), pp. 4516-4522

CrossRef　　View Record in Scopus　　Google Scholar

[24]　The Human Microbiome Project, C, *et al.*
Structure, function and diversity of the healthy human microbiome
Nature, 486 (2012), p. 207

Google Scholar

[25]　The Human Microbiome Project, C, *et al.*
A framework for human microbiome research
Nature, 486 (2012), p. 215

Google Scholar

[26]　K.R. Ludwig, M.M. Schroll, A.B. Hummon
Comparison of in-solution, FASP, and S-trap based digestion methods for bottom-up proteomic studies
J. Proteome Res., 17 (7) (2018), pp. 2480-2490

CrossRef　　View Record in Scopus　　Google Scholar

[27]　Gene [Internet]
Bethesda (MD): National Library of Medicine (US), National Center for Biotechnology Information
[cited 2019 Nov 17]. Available from
https://www.ncbi.nlm.nih.gov/gene/ (2004)

Google Scholar

[28]　Y. Cheng, *et al.*
LMO3 promotes hepatocellular carcinoma invasion, metastasis and anoikis inhibition by directly interacting with LATS1 and suppressing hippo signaling
J. Exp. Clin. Cancer Res., 37 (1) (2018), Article 228

CrossRef　　View Record in Scopus　　Google Scholar

[29]　J. Deng, *et al.*
LATS1 suppresses proliferation and invasion of cervical cancer
Mol. Med. Rep., 15 (4) (2017), pp. 1654-1660

CrossRef　　View Record in Scopus　　Google Scholar

≡ **Outline**   📄 **Download**   **Share**   **Export**

oncoprotein in non-small-cell lung cancer

Tumour Biol., 35 (7) (2014), pp. 6435-6443

CrossRef   View Record in Scopus   Google Scholar

[31]   T. Yu, J. Bachman, Z.C. Lai

Mutation analysis of large tumor suppressor genes LATS1 and LATS2 supports a tumor suppressor role in human cancer

Protein Cell, 6 (1) (2015), pp. 6-11

CrossRef   View Record in Scopus   Google Scholar

[32]   H. Feng, *et al.*

Downregulated expression of CFHL1 is associated with unfavorable prognosis in postoperative patients with hepatocellular carcinoma

Exp. Ther. Med., 17 (5) (2019), pp. 4073-4079

View Record in Scopus   Google Scholar

[33]   B. Zhang, H. Wu

Decreased expression of COLEC10 predicts poor overall survival in patients with hepatocellular carcinoma

Cancer Manag. Res., 10 (2018), pp. 2369-2375

View Record in Scopus   Google Scholar

[34]   Y. Wei, *et al.*

Identification of 1,4-galactosyltransferase I as a target gene of HBx-induced cell cycle progression of hepatoma cell

J. Hepatol., 49 (6) (2008), pp. 1029-1037

Article   📄 Download PDF   View Record in Scopus   Google Scholar

[35]   X. Zhu, *et al.*

Elevated β1,4-galactosyltransferase I in highly metastatic human lung cancer cells: identification of E1AF as important transcription activator

J. Biol. Chem., 280 (13) (2005), pp. 12503-12516

View Record in Scopus   Google Scholar

[36]   H.-J. Choi, *et al.*

Estrogen induced β-1,4-galactosyltransferase 1 expression regulates proliferation of human breast cancer MCF-7 cells

Biochem. Biophys. Res. Commun., 426 (4) (2012), pp. 620-625

Article   📄 Download PDF   View Record in Scopus   Google Scholar

[37]   H. Zhou, *et al.*

☰ Outline   📄 Download   Share   Export

FEBMS Life, 64 (11) (2012), pp. 889-900

CrossRef   View Record in Scopus   Google Scholar

[38]   M. Li, *et al.*

ASAP1 mediates the invasive phenotype of human laryngeal squamous cell carcinoma to affect survival prognosis

Oncol. Rep., 31 (6) (2014), pp. 2676-2682

CrossRef   View Record in Scopus   Google Scholar

[39]   T. Hou, *et al.*

Overexpression of ASAP1 is associated with poor prognosis in epithelial ovarian cancer

Int. J. Clin. Exp. Pathol., 7 (1) (2013), pp. 280-287

View Record in Scopus   Google Scholar

[40]   T. Zhang, *et al.*

Overexpression of flavin-containing monooxygenase 5 predicts poor prognosis in patients with colorectal cancer

Oncol. Lett., 15 (3) (2018), pp. 3923-3927

View Record in Scopus   Google Scholar

[41]   Y. Pan, *et al.*

Endoplasmic reticulum ribosome-binding protein 1, RRBP1, promotes progression of colorectal cancer and predicts an unfavourable prognosis

Br. J. Cancer, 113 (5) (2015), pp. 763-772

CrossRef   View Record in Scopus   Google Scholar

[42]   S. Liu, *et al.*

RRBP1 overexpression is associated with progression and prognosis in endometrial endometrioid adenocarcinoma

Diagn. Pathol., 14 (1) (2019), Article 7

View Record in Scopus   Google Scholar

[43]   D. Broccoli, *et al.*

Human telomeres contain two distinct Myb–related proteins, TRF1 and TRF2

Nat. Genet., 17 (2) (1997), pp. 231-235

CrossRef   Google Scholar

[44]   P.G. Kaminker, *et al.*

TANK2, a new TRF1-associated poly(ADP-ribose) polymerase, causes rapid induction of cell death upon overexpression

J. Biol. Chem., 276 (38) (2001), pp. 35891-35899

Cloning and characterization of TNKL, a member of tankyrase gene family
Genes Immun., 2 (1) (2001), pp. 52-55
CrossRef   View Record in Scopus   Google Scholar

[46]   N. Sidorova, *et al.*
Immunohistochemical detection of tankyrase 2 in human breast tumors and normal renal tissue
Cell Tissue Res., 323 (1) (2006), pp. 137-145
CrossRef   View Record in Scopus   Google Scholar

[47]   D. Yang, *et al.*
HUWE1 controls the development of non-small cell lung cancer through down-regulation of p53
Theranostics, 8 (13) (2018), pp. 3517-3529
View Record in Scopus   Google Scholar

[48]   S. Confalonieri, *et al.*
Alterations of ubiquitin ligases in human cancer and their association with the natural history of the tumor
Oncogene, 28 (33) (2009), pp. 2959-2968
CrossRef   View Record in Scopus   Google Scholar

[49]   M. Masià-Balagué, *et al.*
Gastrin-stimulated Gα13 activation of Rgnef protein (ArhGEF28) in DLD-1 colon carcinoma cells
J. Biol. Chem., 290 (24) (2015), pp. 15197-15209
CrossRef   View Record in Scopus   Google Scholar

[50]   L. Castéra, *et al.*
Landscape of pathogenic variations in a panel of 34 genes and cancer risk estimation from 5131 HBOC families
Genet. Med., 20 (12) (2018), pp. 1677-1686
CrossRef   View Record in Scopus   Google Scholar

[51]   F. Brellier, *et al.*
SMOC1 is a tenascin-C interacting protein over-expressed in brain tumors
Matrix Biol., 30 (3) (2011), pp. 225-233
Article   📕 Download PDF   View Record in Scopus   Google Scholar

[52]   G.W. Rhyasen, D.T. Starczynowski

Outline   Download   Share   Export

CrossRef   View Record in Scopus   Google Scholar

[53]   Q. Xie, *et al.*
Loss of the innate immunity negative regulator IRAK-M leads to enhanced host immune defense against tumor growth
Mol. Immunol., 44 (14) (2007), pp. 3453-3461
Article   Download PDF   View Record in Scopus   Google Scholar

[54]   X. Xiao, *et al.*
Role of MUC20 overexpression as a predictor of recurrence and poor outcome in colorectal cancer
J. Transl. Med., 11 (2013), p. 151
CrossRef   Google Scholar

[55]   C.-H. Chen, *et al.*
MUC20 overexpression predicts poor prognosis and enhances EGF-induced malignant phenotypes via activation of the EGFR-STAT3 pathway in endometrial cancer
Gynecol. Oncol., 128 (3) (2013), pp. 560-567
Article   Download PDF   View Record in Scopus   Google Scholar

[56]   C.-H. Chen, *et al.*
MUC20 promotes aggressive phenotypes of epithelial ovarian cancer cells via activation of the integrin β1 pathway
Gynecol. Oncol., 140 (1) (2016), pp. 131-137
Article   Download PDF   View Record in Scopus   Google Scholar

[57]   S. Sivasubramaniam, *et al.*
Cep164 is a mediator protein required for the maintenance of genomic stability through modulation of MDC1, RPA, and CHK1
Genes Dev., 22 (5) (2008), pp. 587-600
CrossRef   View Record in Scopus   Google Scholar

[58]   Y.-R. Pan, E.Y.H.P. Lee
UV-dependent interaction between Cep164 and XPA mediates localization of Cep164 at sites of DNA damage and UV sensitivity
Cell Cycle, 8 (4) (2009), pp. 655-664
CrossRef   View Record in Scopus   Google Scholar

[59]   J. Delezie, *et al.*
The nuclear receptor REV-ERBα is required for the daily balance of carbohydrate and lipid metabolism

[60]   B. Pourcet, *et al.*
Nuclear receptor subfamily 1 group d member 1 regulates circadian activity of NLRP3 inflammasome to reduce the severity of fulminant hepatitis in mice
Gastroenterology, 154 (5) (2018)
1449–1464 e20
Google Scholar

[61]   L. Dini, *et al.*
The clearance of apoptotic cells in the liver is mediated by the asialoglycoprotein receptor
FEBS Lett., 296 (2) (1992), pp. 174-178
Article   📄 Download PDF   View Record in Scopus   Google Scholar

[62]   C.S. Guy, S.L. Rankin, T.I. Michalak
Hepatocyte cytotoxicity is facilitated by asialoglycoprotein receptor
Hepatology, 54 (3) (2011), pp. 1043-1050
CrossRef   View Record in Scopus   Google Scholar

[63]   J.B. Burgess, J.U. Baenziger, W.R. Brown
Abnormal surface distribution of the human asialoglycoprotein receptor in cirrhosis
Hepatology, 15 (4) (1992), pp. 702-706
CrossRef   View Record in Scopus   Google Scholar

[64]   S.R. Dalton, *et al.*
Carbon tetrachloride-induced liver damage in asialoglycoprotein receptor-deficient mice
Biochem. Pharmacol., 77 (7) (2009), pp. 1283-1290
Article   📄 Download PDF   View Record in Scopus   Google Scholar

[65]   S.L. Leber, *et al.*
Homer1a protein expression in schizophrenia, bipolar disorder, and major depression
J. Neural Transm. (Vienna), 124 (10) (2017), pp. 1261-1273
CrossRef   View Record in Scopus   Google Scholar

[66]   P. Luo, *et al.*
Scaffold protein Homer 1: implications for neurological diseases
Neurochem. Int., 61 (5) (2012), pp. 731-738
Article   📄 Download PDF   View Record in Scopus   Google Scholar

[67]   K.K. Szumlinski, *et al.*
Behavioral and neurochemical phenotyping of Homer1 mutant mice: possible relevance to schizophrenia

≡ Outline   📄 Download   Share   Export

[68] C.A. Dickey, *et al.*

Selectively reduced expression of synaptic plasticity-related genes in amyloid precursor protein + presenilin-1 transgenic mice

J. Neurosci., 23 (12) (2003), pp. 5219-5226

CrossRef   View Record in Scopus   Google Scholar

[69] C. Ménard, R. Quirion

Successful cognitive aging in rats: a role for mGluR5 glutamate receptors, Homer 1 proteins and downstream signaling pathways

PLoS One, 7 (1) (2012), Article e28666

CrossRef   Google Scholar

[70] C. Visconte, *et al.*

Amyloid precursor protein is required for in vitro platelet adhesion to amyloid peptides and potentiation of thrombus formation

Cell. Signal., 52 (2018), pp. 95-102

Article   📄 Download PDF   View Record in Scopus   Google Scholar

[71] S.J. Furney, *et al.*

Genome-wide association with MRI atrophy measures as a quantitative trait locus for Alzheimer's disease

Mol. Psychiatry, 16 (11) (2011), pp. 1130-1138

CrossRef   View Record in Scopus   Google Scholar

[72] E.K. Green, *et al.*

Association at SYNE1 in both bipolar disorder and recurrent major depression

Mol. Psychiatry, 18 (5) (2013), pp. 614-617

CrossRef   View Record in Scopus   Google Scholar

[73] M.A. Geeves, S.E. Hitchcock-DeGregori, P.W. Gunning

A systematic nomenclature for mammalian tropomyosin isoforms

J. Muscle Res. Cell Motil., 36 (2) (2015), pp. 147-153

CrossRef   View Record in Scopus   Google Scholar

[74] N. Vlahovich, *et al.*

Tropomyosin 4 defines novel filaments in skeletal muscle associated with muscle remodelling/regeneration in normal and diseased muscle

Cell Motil. Cytoskeleton, 65 (1) (2008), pp. 73-85

CrossRef   View Record in Scopus   Google Scholar

J. Cell Sci., 128 (10) (2015), pp. 2965-2974

CrossRef   View Record in Scopus   Google Scholar

[76]   L. Blanchoin, *et al.*

Actin dynamics, architecture, and mechanics in cell motility

Physiol. Rev., 94 (1) (2014), pp. 235-263

CrossRef   View Record in Scopus   Google Scholar

[77]   A.J. Kee, *et al.*

An actin filament population defined by the tropomyosin Tpm3.1 regulates glucose uptake

Traffic, 16 (7) (2015), pp. 691-711

CrossRef   View Record in Scopus   Google Scholar

[78]   C.Y. Lim, *et al.*

Tropomodulin3 is a novel Akt2 effector regulating insulin-stimulated GLUT4 exocytosis through cortical actin remodeling

Nat. Commun., 6 (2015), Article 5951

Google Scholar

[79]   Z. Liu, *et al.*

The role of cytoskeleton in glucose regulation

Biochemistry (Mosc), 71 (5) (2006), pp. 476-480

View Record in Scopus   Google Scholar

[80]   S.A. Dunn, *et al.*

Altered tropomyosin expression in essential hypertension

Hypertension, 41 (2) (2003), pp. 347-354

View Record in Scopus   Google Scholar

[81]   M. Nematy, *et al.*

Effects of Ramadan fasting on cardiovascular risk factors: a prospective observational study

Nutr. J., 11 (2012), p. 69

Google Scholar

[82]   A.I. Al-Shafei

Ramadan fasting ameliorates arterial pulse pressure and lipid profile, and alleviates oxidative stress in hypertensive patients

Blood Press., 23 (3) (2014), pp. 160-167

CrossRef   View Record in Scopus   Google Scholar

☰ **Outline**   📄 **Download**   **Share**   **Export**

Trends Cell Biol., 5 (11) (1995), pp. 381-385

Article   📄 Download PDF   View Record in Scopus   Google Scholar

[84]   Z. Ding, *et al.*

Both actin and polyproline interactions of profilin-1 are required for migration, invasion and capillary morphogenesis of vascular endothelial cells

Exp. Cell Res., 315 (17) (2009), pp. 2963-2973

Article   📄 Download PDF   View Record in Scopus   Google Scholar

[85]   K.T. Dalen, *et al.*

Adipose tissue expression of the lipid droplet-associating proteins S3-12 and perilipin is controlled by peroxisome proliferator-activated receptor-gamma

Diabetes, 53 (5) (2004), pp. 1243-1252

CrossRef   View Record in Scopus   Google Scholar

[86]   A.M. Sharma, B. Staels

Peroxisome proliferator-activated receptor γ and adipose tissue—understanding obesity-related changes in regulation of lipid and glucose metabolism

J. Clin. Endocrinol. Metab., 92 (2) (2007), pp. 386-395

CrossRef   View Record in Scopus   Google Scholar

[87]   T.T. Chiu, *et al.*

Arp2/3- and cofilin-coordinated actin dynamics is required for insulin-mediated GLUT4 translocation to the surface of muscle cells

Mol. Biol. Cell, 21 (20) (2010), pp. 3529-3539

View Record in Scopus   Google Scholar

[88]   W. Qi, *et al.*

Pyruvate kinase M2 activation may protect against the progression of diabetic glomerular pathology and mitochondrial dysfunction

Nat. Med., 23 (6) (2017), pp. 753-762

CrossRef   View Record in Scopus   Google Scholar

[89]   S.M. Grundy, *et al.*

Diagnosis and management of the metabolic syndrome: an American Heart Association/National Heart, Lung, and Blood Institute Scientific Statement

Circulation, 112 (17) (2005), pp. 2735-2752

View Record in Scopus   Google Scholar

[90]   G. Marchesini, R. Marzocchi

Metabolic syndrome and NASH

Article   Download PDF   View Record in Scopus   Google Scholar

[91]   I. Labayen, *et al.*

Basal and postprandial substrate oxidation rates in obese women receiving two test meals with different protein content

Clin. Nutr., 23 (4) (2004), pp. 571-578

Article   📄 Download PDF   View Record in Scopus   Google Scholar

[92]   K.J. Motil, *et al.*

Leucine oxidation changes rapidly after dietary protein intake is altered in adult women but lysine flux is unchanged as is lysine incorporation into VLDL-apolipoprotein B-100

J. Nutr., 124 (1) (1994), pp. 41-51

View Record in Scopus   Google Scholar

[93]   D.J. Harney, *et al.*

Proteomic analysis of human plasma during intermittent fasting

J. Proteome Res., 18 (5) (2019), pp. 2228-2240

CrossRef   View Record in Scopus   Google Scholar

ELSEVIER

About ScienceDirect

Remote access

Shopping cart

Advertise

Contact and support

Terms and conditions

Privacy policy

℞ RELX™